THE PUBLISHING HOUSE
OF THE ROMANIAN ACADEMY

PROCEEDINGS OF THE ROMANIAN ACADEMY, Series A,
Volume 18, Number 4/2017, pp. 361–369

DYNAMIC AND QUASI-STATIC COMPRESSION TESTS OF CLOSED-CELL ALUMINIUM ALLOY FOAMS

Emanoil LINUL[1], Liviu MARSAVINA[1], Jaroslav KOVACIK [2], Tomasz SADOWSKI [3]

[1] "Politehnica" University of Timisoara, Department of Mechanics and Strength of Materials,
1 Mihai Viteazu Avenue, 300 222 Timisoara, Romania
[2] Slovak Academy of Science, Institute of Materials & Machine Mechanics SAS,
Račianska 75 str., 831 02, Bratislava 3, Slovakia
[3] Lublin University of Technology, Department of Solid Mechanics, Nadbystrzyka 40 str.,
20–618 Lublin, Poland
Corresponding author: Liviu MARSAVINA, E-mail: liviu.marsavina@upt.ro

Abstract. A mechanical characterization of closed-cell aluminium foams (AlSi12Mg0.6) prepared by powder metallurgy route under quasi-static and dynamic compressive loading was investigated. Cellular structure of some samples was evaluated using computer image analysis prior compression tests. The experimental tests were carried out on half-cylindrical specimens with surface skin in the density range of 350–550 kg/m^3 (Note: one half of cylindrical specimen was used for quasi-static tests and other one for dynamic tests, thus having almost identical structure). The compression tests were performed with crosshead speed of $1.67.10^{-4}$ m/s for quasi-static and 3.72 m/s for dynamic tests. Based on the experimental data, a linear correlation between quasi-static and dynamic compressive strength at 20% and 50% strain is proposed. Obvious connection between strain rate, some properties of stress-strain curve and microstructure was observed.

Key words: aluminium foams, quasi-static/dynamic compression tests, mechanical properties.

1. INTRODUCTION

The mechanical properties of cellular materials such as metallic and polyurethane foams depend directly on those of the solid material from they are made and their relative density; but they are influenced also by its cell topology (open/closed cell), cell size and cell shape [1–3].

It is well-know that metallic foams, especially those made from aluminium and its alloys are being widely used in a number of critical applications. Excellent stiffness-to-weight ratio, low density, good shear and fracture strength, the damping capacity, higher natural flexural vibration frequency and sound-absorbing capacity makes foams ideal for lightweight structures, sandwich cores, isolation, mechanical damping devices, vibration control, acoustic absorption, biocompatible inserts, electrical screening, heat exchangers and filters [4–6]. This extensive applicability of aluminium foams are direct consequence of their cellular structure.

However, studies on the deformation and fracture of aluminium foams are still in their infancy, compared to conventional materials such as 'regular' metals. A significant part of the necessary theoretical and experimental framework is not yet fully developed for this class of materials, even though extensive works have been carried out in this field [7–12].

The compressive behaviour of three different cellular aluminium alloys in a wide range of density has been investigated by Montanini [7] under quasi-static and dynamic loading. The results reported in this study showed that strain rate sensitivity can be considered negligible for open-cell morphology, while it is significant for closed-cell foams.

Liu *et al*. [8] studied two different aluminium foams, manufactured by molten body transitional foaming process with the aim of explaining the impact behaviour, deformation mode and energy absorbing ability.

Mechanical effects of mass density gradients in metallic foams have been investigated experimentally under combined compression and shear deformation by [9]. The results show that two distinct crushing modes characterize the energy absorption of foams depending on compression or shear dominance.

Song *et al*. [10] determined the mechanical properties of brittle aluminium foams under compressive conditions. Tests on specially designed small samples were accomplished in a loading device equipped in the scanning electron microscopy. They found four failure modes in the cell-wall level (Mode I-compressive bending and fracturing; Mode II-direct brittle fracture due to tension or shearing; Mode III-cracking in the cell face, due to stretching induced from remote compressive stress, when the cell face parallels the compression axis and Mode IV-shear and friction between fractured cell walls, usually occurs at high compressive strains) and these modes account for the mesoscopic mechanisms of energy absorption.

The quasi-static and dynamic compression for closed-cell aluminium foams with relative density ranging from 0.06 to 0.4 was studied by Raj *et al*. [11]. The results of the study indicated that the plateau stress of aluminium foam increases with relative density and strain rate. Additionally, at high strain rates, an increase in the energy absorption capacity was observed.

Saadatfar *et al*. [12] characterize four metallic foam samples manufactured under various experimental conditions. They used X-ray tomography to study 3D structure of the foam samples. They characterized cell shape and size and attempt to correlate them with the manufacturing parameters.

Figure 1 presents the inner cellular structure of investigated foams for three different densities.

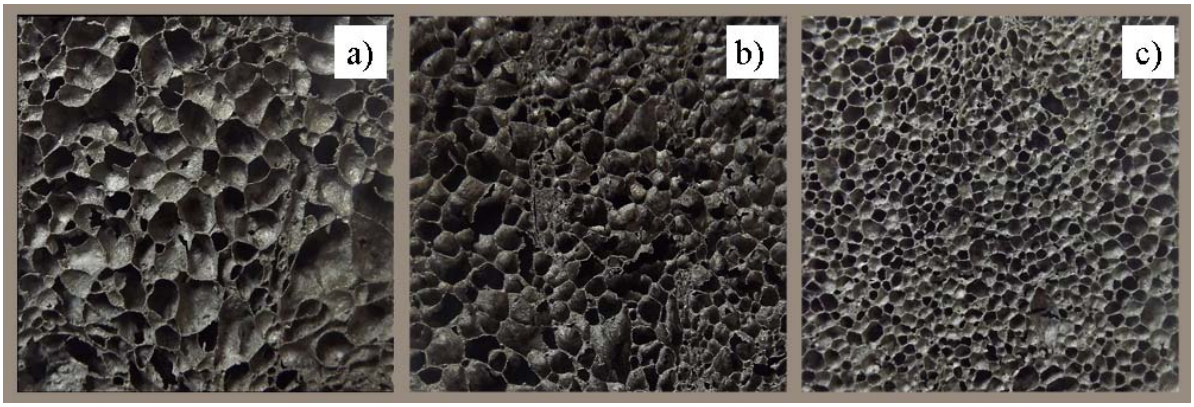

Fig. 1 – Cellular structure of investigated Al foams:
a) $\rho = 350$ kg/m^3 b) $\rho = 423$ kg/m^3 c) $\rho = 550$ kg/m^3.

Modelling and predicting of the behaviour of Al foams requires the detailed knowledge of their structures mechanical response. The problem is stochastic character of foam structure. Therefore the main aim of this paper is to investigate the compression properties of brittle closed-cells Al foams with surface skin prepared by powder metallurgy route under various strain rates ***at almost constant pore structure***.

2. STATISTIC ANALYSIS OF THE CLOSED-CELL FOAM MICROSTRUCTURE

Before QS and D compression tests some samples were polished and then sprayed black to observe the microstructure of foams before tests. The structures were scanned to computer and quantitative evaluation of the aluminium foam structure was performed using the computer software Image Pro Plus (Media Cybernetics Inc., USA). This software makes the determination of following structural parameters possible: (i) square fraction of the pore walls in the selected location (local density of the aluminium foam); (ii) number of pores in the selected area; (iii) area of pores in the selected location and its distribution into predefined classes; (iv) apparent diameter of pores and their distribution into predefined classes; (v) shape of pores defined by the ratio of major and minor axis of an equivalent ellipse (aspect ratio), i.e. the ellipse with the same area than the investigated pore; (vi) pore orientation, determined by the angle between the orientation of the major axis of the equivalent ellipse and the vertical axis of the section image.

Example of such statistical evaluation for half-cylindrical aluminium foam AlSi12Mg0.6 samples with diameter 40 mm, height 51 mm, sample density 408 kg/m^3 is shown in Fig. 2.

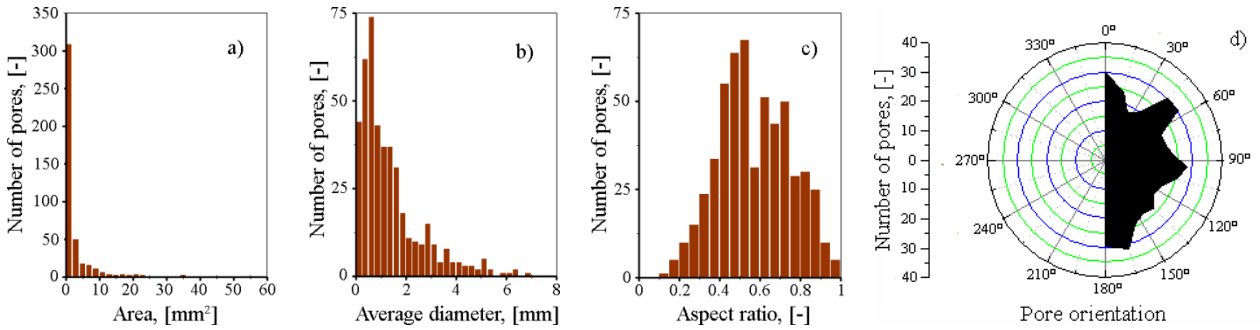

Fig. 2 – Distribution of pore area (a), average diameter (b), aspect ratio (c) and pore orientation (d) for half-cylindrical specimen.

It is evident that the pore area and average diameter size distribution is noised by small pores existing within the structure. Therefore, the probability to be within the pore of certain size when randomly point into the structure was used to determine the average pore size of 4.5 mm. From other two diagrams it is evident that the pores are not spherical at all with maximum of aspect ratio (length of minor to major equivalent ellipse) at 0.5 and 0.7 with preferred orientation at 0, 45 and 90 degrees with respect to vertical axis of the structure (Fig. 3).

It was already proposed [13] that the foam breaks at pore layer with highest porosity or lowest density. To check this idea, the foam structure was divided into the 10 independent regions (perpendicular to the expected direction of compression) of constant width and the image density was calculated in every region and the position of most porous region was found between 15–20 mm from sample bottom (Fig. 3).

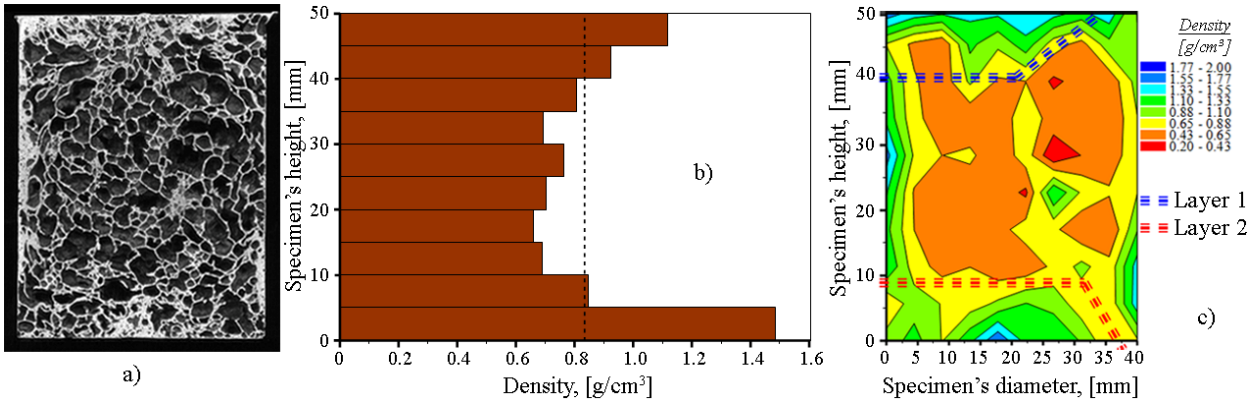

Fig. 3 – Local distribution of image density in bands perpendicular to applied force during compression (width of bands approx. 5 mm) – sample density 408 kg/m^3.

The strain field on the surface of metallic foams resulting from mechanical loading can be measured also using a technique known as surface strain mapping. The surfaces of cellular metals are irregular, with the cell membranes appearing as peaks and troughs, allowing in-situ optical imaging to be used to provide a map of surface deformation [1]. The precise investigation showed that the real structural damage was more complex. The damaged part was not simply inside of the weakest pore layer perpendicular to applied force. Approximately 1/3 of its length deviates from this into more dense part. It was proposed that the investigated picture ought to be more complex and image density distribution was calculated for 100 rectangles full covering original structure. Image density distribution plot inside of sample according to division of original picture into the 100 squares 4 × 5 mm^2 are presented in Fig. 3. Legend shows the variations of image density from 200 to 2 000 kg/m^3. Density surface plot at Fig. 9 confirmed two possible deviation paths from weakest layer (Layer 1 and Layer 2). But, before compression test one cannot decide which of the two possible directions will be favoured by crack propagation.

As confirmed the observation of the foam sample structure changes during compression tests the weakest layer determined by image analysis really breaks the first (Fig. 4). Behaviour of the investigated

foam structure under quasi-static compression test is presented in Fig. 4 as follows: 0% strain with marked broken layer before compressive yield point up to 41 % strain.

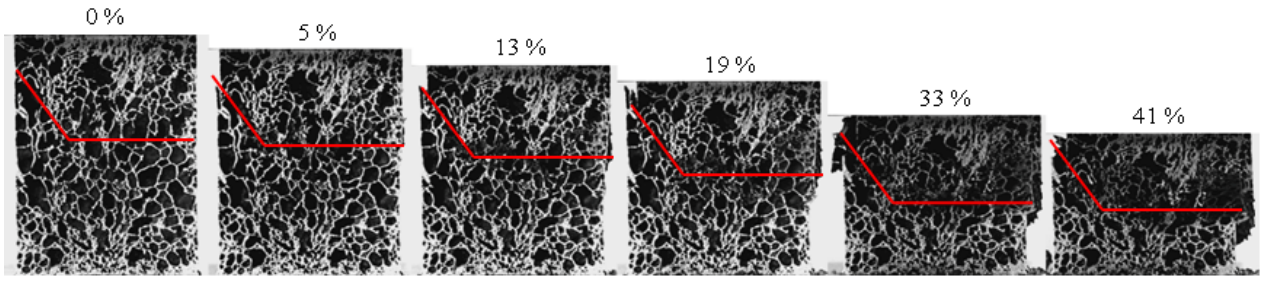

Fig. 4 – Foam structure for different strains with marked broken weakest layer (foam density 399 kg/m^3).

3. EXPERIMENTAL INVESTIGATIONS

This work presents a mechanical characterization of AlSi12Mg0.6 closed-cell aluminium foams under quasi-static (QS) and dynamic (D) compressive loading. The testing specimens were manufactured by powder metallurgy route (PMR) method at IMMM SAS, Bratislava, Slovakia. The composition of the cell wall material is: 87.6 wt. % AlSi12; 12 wt. % AlMg5 and 0.4% TiH_2 as foaming agent (Alulight foams in older literature). Cylindrical samples with diameter of 40 mm and length of 51 mm were prepared. Then the samples were cut by electric discharge machining and one half was used for QS tests and the other one for D tests ***thus having almost identical structure, and almost same density.*** It must be pointed out that Because of the cellular structure, pore size, wall thickness the maximally 8% density difference between the two halves of original sample was observed for all investigated samples. QS and D tests were carried out on half-cylindrical specimens with original surface skin (thickness between 0.09–0.24 mm) – the only exception was cutting plane. Investigated foams had densities in the range of 350–550 kg/m^3.

QS tests were performed at IMMM SAS using a 15kN Instron testing machine, while the dynamic (D) compression tests were carried on the Strength of Materials Laboratory from Lublin University of Technology, Poland using a 40 kN Instron-Dynatup impact testing machine (Fig. 5). The load was measured by the load cell of the test machine and the machine platen displacement was used to define the axial strain in the specimen. The experimental tests were performed at room temperature (23°C) with constant crosshead speed of $1.67 \cdot 10^{-4}$ m/s for QS tests and 3.72 m/s for D tests. The tests were performed according to [14].

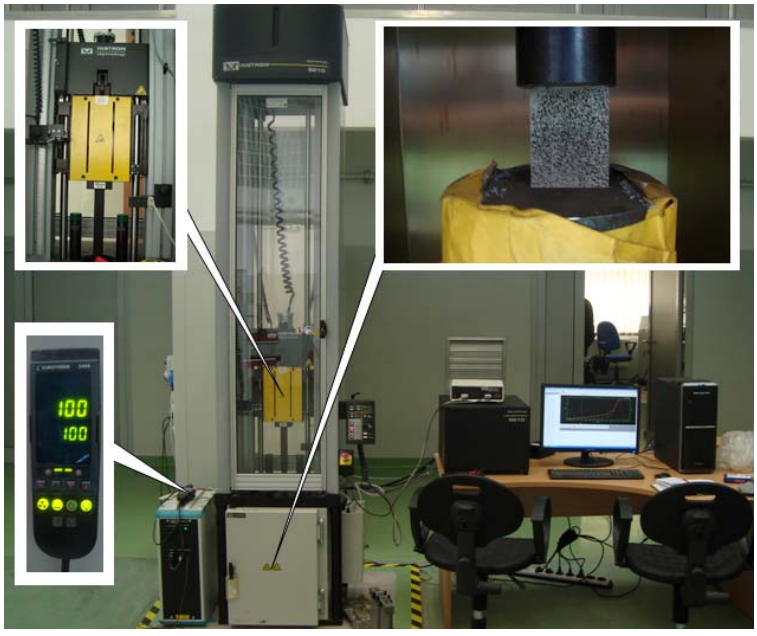

Fig. 5 – 40 kn Dynamic Instron – Dynatup testing machine.

Since the foam's mechanical properties are largely dependent on its density, a set of QS and D tests were conducted on foam samples in order to determine the effect of the foam's density on their mechanical properties. After testing the stress-strain curves were obtained. In this respect Fig. 6 presents the uniaxial compressive responses for different densities of closed-cell aluminum foams under QS respectively D compressive tests. Both figures show an increase of mechanical properties with increasing density.

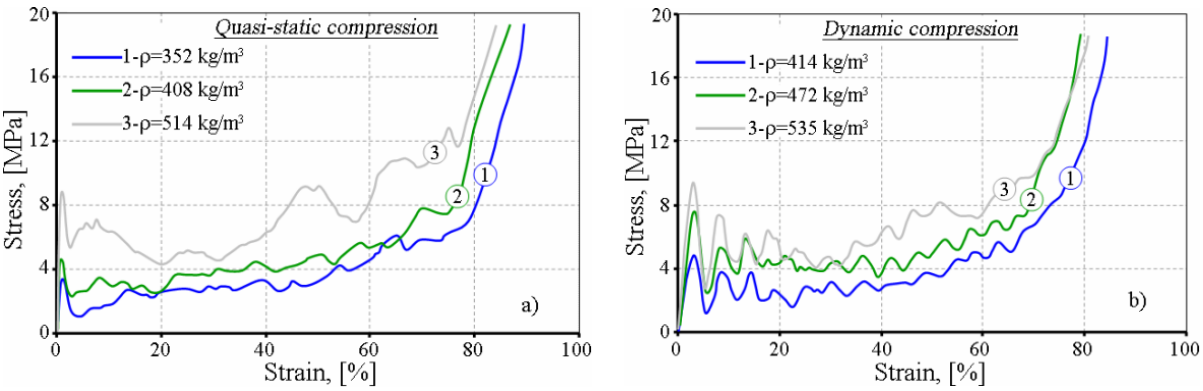

Fig. 6 – Stress-strain curves from QS (a) and D (b) compression tests on a half-cylindrical specimen of used aluminum foam.

The trend of the curves is quite repeatable and is mainly characterized by sharp oscillations for D tests, produced by the progressive brittle fracture of cells belonging to different almost parallel planes [7].

4. RESULTS AND DISCUSSIONS

The results are reported in terms of the stress-strain curves during compression up to approximately 90% engineering strain. As generally observed on cellular materials [1, 15], the compressive stress–strain curve of cellular materials exhibit three definite regions / zones: almost linear elastic region (between zero stress - compressive yield stress), constant plateau region (between compressive yield stress - densification strain) and densification region (after densification strain) regardless strain rate serrations. These regions are also clearly observable on Fig. 6. Compressive stress increased with increasing strain almost linearly until an apparent low strain 5%, accompanied by the overall elastic deformation of the cell walls. Apparent Young's Modulus is determined from this linear-elastic region and it occurs due to cell face stretching and cell face bending [16]. The obvious defects in the cell wall induced further local stress concentration and weakened the wall strength. As a result we obtain the first point on the stress-strain diagram from which an increase in strain occurs without an increase in stress defined as the compressive yield stress, σ_y.

As the load increases, the foam cells begin to collapse by elastic buckling, brittle crushing and brittle shear due to rotation of cell walls. At higher strains, plastic hinges form in the cell faces and fail in bending fracture. After breaking of the first cell, in its vicinity begun to yield other cells, due to the stress redistribution after first cell face fracture. The stress level is appreciably high at this stage, and both fracturing, shear and yielding of faces contribute to this high stress. For many types of cellular materials, the plateau regime starts from the compressive yield strain, ε_y, or compressive yield stress, σ_y, representing the initiation of the new deformation mechanism of the cell face or the cell face failure, and ends at a densification strain, ε_D, representing the onset of densification [17].

Finally, cell faces lose their integrity and the fractured fragments tended to be compacted, causing a notable increase in stress. Two opposing cell faces begun to contact indicating a further compaction. The stress increased continuously and steeply to a limiting strain known as densification. The onset strain of densification is defined as the strain at which the slope of the curve in a plot of energy efficiency (η) versus strain (ε) is zero. The onset strain of densification for cellular solids represents the start of the cell wall interactions, which enhance the compressive resistance of a cellular solid [10, 16–18].

The observed results for the investigated foams are consistent with findings already observed in literature [15, 19, 20]. Basically it higher compressive yield stress and shorter plateau region for higher strain rates was observed. The almost identical structure enabled us to investigate the effect of the structure of foam

on stress-strain curve for various strain rates. We have focused on the analysis of the 1st stress drop of QS and D tests. The obtained analysis for various densities of studied foams is listed in Table 1 and Table 2, where D_p is apparent pore diameter, l_p is deformation in mm corresponding to the 1st stress drop.

Table 1

The 1st stress drop results for quasi-static compression tests

Spec. No.	Density	D_p	σ_y	PS	ε_D	ε_y	1st minima	strain@1st minima	Δstrain	Δstress	l_p	l_p/D_p	$\Delta s/\sigma_y$
	[kg/m^3]	[mm]	[MPa]	[MPa]	[%]	[%]	[MPa]	[%]	[MPa]	[%]	[mm]	[%]	[%]
1	350	6.02	3.41	2.84	49.18	1.215	0.98	4.605	2.43	3.39	1.732	28.8	71.26
2	373	3.87	4.34	2.17	48.54	1.332	1.77	3.870	2.57	2.538	1.299	33.6	59.22
3	399	3.90	5.67	2.47	43.16	1.471	3.01	3.005	2.66	1.534	0.767	19.7	46.91
4	408	3.96	4.61	2.90	64.33	1.017	2.29	2.860	2.32	1.843	0.942	23.8	50.33
5	423	2.92	5.44	2.85	46.78	1.150	3.20	2.556	2.24	1.406	0.720	24.6	41.18
6	514	3.03	8.90	4.14	50.18	1.087	5.27	2.620	3.63	1.533	0.785	25.9	40.79
7	513	4.66	7.26	4.79	57.83	1.079	3.30	4.758	3.96	3.679	1.884	40.4	54.55
average									2.83	2.275	1.161	28.1	52.03
standard deviation									0.68	0.942	0.484	6.9	10.81

Table 2

The 1st stress drop results for dynamic compression tests

Spec. No.	Density	D_p	σ_y	PS	ε_D	ε_y	1st minima	strain@1st minima	Δstrain	Δstress	l_p	l_p/D_p	$\Delta s/\sigma_y$
	[kg/m^3]	[mm]	[MPa]	[MPa]	[%]	[%]	[MPa]	[%]	[MPa]	[%]	[mm]	[%]	[%]
1	404	3.87	6.49	6.49	61.62	3.274	1.95	5.791	4.54	2.52	1.289	33.30	69.95
2	414	3.96	5.06	5.06	53.38	3.308	1.27	5.774	3.79	2.47	1.260	31.79	74.90
3	421	3.03	4.37	4.37	53.28	2.313	1.21	5.715	3.16	3.40	1.742	57.56	72.31
4	468	4.66	6.92	6.92	60.21	3.058	1.49	5.340	5.43	2.28	1.168	25.05	78.47
5	472	2.92	7.60	7.33	53.61	3.260	2.40	5.586	5.20	2.33	1.191	40.72	68.42
6	535	6.02	9.45	10.00	56.78	3.010	2.64	5.370	6.81	2.36	1.206	20.05	72.06
7	550	3.90	10.0	9.45	64.63	3.249	2.22	6.531	7.78	3.28	1.641	42.11	77.80
average									5.24	2.66	1.366	35.75	73.42
standard deviation									1.63	0.47	0.233	12.11	3.81

Similar region was investigated by Peroni *et al*. [21]. However, due to large scatter in pore size, wall thickness and shape of the pores, the density of foams varied considerably. Taking into account the large inhomogeneities of the tested material, the test results are rather scattered and this caused many serious problems in the evaluations of the mechanical properties on effects of density [21].

However, as a general observation it can be said that both quasi-static yield stress and plateau stress values are lower than the dynamic ones with 15–30% approximately. The unique is that for the first time the Al foams prepared by PMR method with surface skins were tested in compression at low and high stain rate (QS and D tests) not only at constant porosity, but also with almost identical structure. Similar tests on almost identical structure were already performed on Alporas aluminium foams however without surface skin (melt route process [22]). For this reason (Fig. 6) large parts of stress-strain curves are identical, similar or of similar manner for both QS and D compression tests. This enabled us not only to observe usual strain rate dependences, such as higher compressive yield stress (σ_y), lower plateau stress (PS), shorter plateau region and earlier densification in the case of dynamic compression, but the following effects were observed:

- The 1st stress drop that occurs after compressive yield stress (σ_y) is 52% of yield stress for QS and 74% for D compression (see values of $\Delta s/\sigma_y$ in Tables 1 and 2) in the investigated density range 350 – 550 kg/m^3. The difference between yield stress for QS and D and also the difference between amplitude of the 1st stress

drop that occurs after yield stress for QS and D tests can be attributed to microinertial effects within the foam. It was already confirmed that the strain rate dependence of matrix material and entrapped gas within pores can be neglected for aluminium foams [22].

- The same decrease of σ_y has the origin in the materials properties, sample geometry and also in the thickness of surface skin already present on PM prepared aluminium foams. In this case the foam can be modelled as outer metallic tube of certain thickness (thickness of surface skin) filled with foam core (varying porosity). Within the investigated porosity range the foam inner core is significantly porous, thus porosity variations can be neglected and the predominant role plays in this case the surface skin thickness which leads to almost constant percentage decrease from yield stress. Of course, some exceptions can be observed – see sample 1 for QS loading in Table 1.
- It was originally proposed [23] that the strain interval corresponding to the 1st stress drop that occurs after yield stress, depends predominantly on the structure of foam, especially apparent pore diameter (pore size that can be most probably find within foam structure). If we continue with our model, after yield stress the surface skin and foam inner core are already broken. The possible deformation (similar to plastic hinging of aluminium tubes) cannot be governed by outer diameter of sample in this case. Therefore it is characteristic pore size of foam inner core that is controlling maximal possible deformation of sample prior to further increase of stress. Basically, it is the pore size of weakest pore layer (Fig. 3). Therefore in the first approximation the dependence of the strain interval corresponding to the 1st stress drop on the apparent pore diameter was investigated more carefully for quasi static samples and the same apparent pore diameter was used also for evaluation of dynamic tests (assumption of identical structure was used). It was observed that the corresponding strain interval is about 20–36% of observed apparent pore diameter for QS compression. In the case of D compression the corresponding strain interval is 23–49% of apparent pore diameter. It is evident that due to microinertia effects under D tests the whole already broken weakest layer is more rearranged than under QS test. During QS test parts of already broken weakest layer starts to interact earlier, thus preventing further decrease of stress at smaller strain.

It can be concluded, that yield stress and further stress drop are governed by properties of foam matrix material, porosity, sample geometry, thickness of foam surface skin and microinertia effects. This is in the analogy of compression tests on aluminium tubes. However, further deformation, i.e., decreasing stress with increasing strain is governed by foam structure itself and is given by porosity and can be connected to apparent pore diameter of foam structure (the most probable pore within foam structure) for both QS and D compression tests. It must be pointed out, that all of these mechanical properties are strongly dependent on the density (they increase with increasing density).

The plateau region has a high importance in selecting foams for packaging or energy absorption applications. For this reason Table 3 presents the effect of the foam's density on QS and D compressive strength of aluminium foams samples measured at 20% and 50% strain at room temperature [24]. The results for QS and D compressive strength at 20% (Fig. 7a) and 50% strain (Fig. 7b) of the investigated foams are presented. Based on the experimental data, a linear correlation is proposed which could be useful for estimation of dynamic compressive strength if quasi-static compressive strength values are measured in the considered density range (350 to 550 kg/m^3).

Table 3

Dependence of compressive strength at 20% and 50% strain on the foam's density

QS	Density [kg/m^3]	350	373	399	408	423	514	513
	$\sigma_{20\%}$	2.54	2.03	2.55	2.63	3.98	4.33	4.38
	$\sigma_{50\%}$	3.20	2.72	4.53	4.87	5.06	6.29	7.88
D	Density [kg/m^3]	404	414	421	468	472	535	550
	$\sigma_{20\%}$	2.74	2.65	3.26	3.11	4.33	4.13	5.12
	$\sigma_{50\%}$	4.32	3.77	4.30	5.76	4.90	5.49	7.63

The correlation equations (1) and (2) are very important in practical applications for impact energy absorption because the D tests are carried out more difficult than QS ones. In this respect, through these equations the σ_D values can be estimated according to the quasi-static ones which are obtained relatively easily.

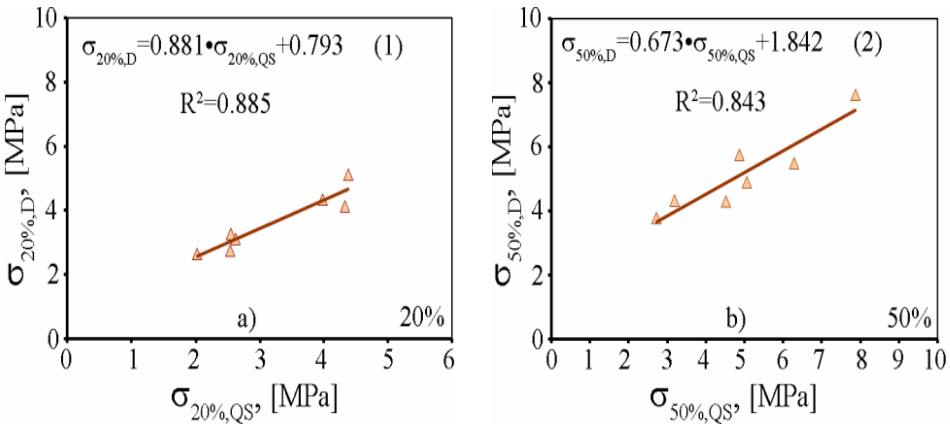

Fig. 7 – Correlation between quasi-static and dynamic compressive strength at 20% (a) and 50% (b).

After QS and D compression tests the foam structure shows a total destruction of cells, which increases the stress delivered to an almost constant strain known as densification. In the moment of densification, due to the filling of the gaps in the foam, this one acts almost like a solid material [25, 26].

5. CONCLUSIONS

The QS and D mechanical characterization of AlSi12Mg0.6 closed-cell aluminium foams with surface skin have been investigated on almost identical structure (half cylindrical specimens prepared from original cylindrical samples by electric discharge machining) to eliminate stochastic effect of foam structures. This enabled us not only to observe usual strain rate dependences, such as higher compressive yield stress (σ_y), lower plateau stress (PS), shorter plateau region and earlier densification in the case of dynamic compression, but the following effects were observed:

- Both, QS and D experimental results showed that the main mechanical properties of aluminium foams increase with increasing of density. The 1st stress drop is about 52% of yield stress for QS and 74% for D compression. This is governed by properties of foam matrix material, porosity, sample geometry, *thickness of foam surface skin* and microinertia effects;
- Corresponding strain interval is about 20–36% of observed apparent pore diameter (most probable pore size within foam structure) for QS compression, while for D compression the corresponding strain interval is around 23–49% of apparent pore diameter. These observations confirmed the assumption, that the strain interval corresponding to 1st stress drop after yield strength is dependent on the structure of foam, especially *apparent pore size* and microinertia effects due to strain rate;
- Based on the experimental data, a linear correlation between QS and D compressive stress at 20% and 50% strain is proposed which could be useful for estimation of dynamic compressive stress if QS compressive stress values are available in the considered density range.
- It was already observed that the foam breaks at weakest pore layer. However, for some samples it was observed that part of the volume of broken layer goes also into the more dense structure of the foam. Image analysis can be used to predict this, but without compression test the favoured way of the crack propagation cannot be determined precisely.

ACKNOWLEDGEMENTS

This work was partially supported by the Grant of the Romanian National Authority for Scientific Research, CNCS-UEFISCDI, project PN-II-ID-PCE-2011-3-0456, contract number 172/2011 and Slovak Grant Agency under contract VEGA 2/0158/13.

The authors are also grateful to colleagues Marcin Knec from Lublin University of Technology and Tudor Voiconi from Politehnica University of Timisoara for their help in performing the experiments.

REFERENCES

1. ASHBY M.F., EVANS A.G., FLECK N.A., GIBSON L.J., HUTCHINSON J.W., *Metal Foams: A Design Guide*, Elsevier Science & Technology Books, 2000.
2. NEGRU R., MARSAVINA L., VOICONI T., LINUL E., FILIPESCU H., BELCIU G., *Application of TCD for brittle fracture of notched PUR materials*, Theoretical and Applied Fracture Mechanics, **80**, Part A, pp. 87–95, 2015.
3. MARSAVINA L., CONSTANTINESCU D.M., LINUL E., VOICONI T., APOSTOL D.A., *Shear and mode II fracture of PUR foams*, Engineering Failure Analysis, **58**, pp. 465–476, 2015.
4. BIRSAN M., SADOWSKI T., MARSAVINA L., LINUL E., PIETRAS D., *Mechanical behavior of sandwich composite beams made of foams and functionally graded materials*, Int. Journal of Solids and Structures, **50**, pp. 519–530, 2013.
5. LINUL E., MARSAVINA L., *Assesment of sandwich beams with rigid polyurethane foam core using failure-mode maps*, Proceedings of the Romanian Academy – Series A, **16**, *4*, pp. 522–530, 2015.
6. VOICONI T., LINUL E., MARSAVINA L., KOVACIK J., KNEC M., *Experimental determination of mechanical properties of aluminium foams using Digital Image Correlation*, Key Engineering Materials, **601**, pp. 254–257, 2014
7. MONTANINI R., *Measurement of strain rate sensitivity of aluminium foams for energy dissipation*, Int. J. of Mech. Sci., **47**, pp. 26–42, 2005.
8. LIU H., CAO Z.K., LUO H.J., SHI J.C., YAO G.C., *Performance of closed-cell aluminum foams subjected to impact loading*, Mat. Sci. Eng. A, **570**, pp. 27–31, 2013.
9. DOYOYO M., MOHR D., *Experimental determination of the mechanical effects of mass density gradient in metallic foams under large multiaxial inelastic deformation*, Mech. of Mat., **38**, pp. 325–339, 2006.
10. SONG H.W., HE Q.J., XIE J.J., TOBOTA A., *Fracture mechanisms and size effects of brittle metallic foams: In situ compression tests inside SEM*, Comp. Sci. and Techn., **68**, pp. 2441–2450, 2008.
11. RAJ E.R., PARAMESWARAN V., DANIEL B.S.S., *Comparison of quasi-static and dynamic compression behavior of closed-cell aluminum foam*, Mat. Sci. Eng. A, **526**, pp. 11–15, 2009.
12. SAADATFAR M., GARCIA-MORENOB F., HUTZLER S., SHEPPARD A.P., KNACKSTEDT M.A., *Imaging of metallic foams using X-ray micro-CT, Colloids and Surfaces A: Physicochem*. Eng. Aspects, **344**, pp. 107–112, 2009.
13. SIMANČÍK F., *Reproducibility of aluminium foam properties*. In: Int. Conf. on Metal Foams and Porous Metal Structures, 14–16 June 99 Bremen, Eds. J. Banhart, M.F. Ashby, N.A. Fleck, MIT Publishing, Bremen, pp. 235–240.
14. KANETAKE N., HIPKE T., MIYOSHI T., NAKAJIMA H., ONO F., KRUPP U., *International Standard for Compression Test of Porous and Cellular Metals*, Proc. of the 6th Int. Conf. on Porous Metals and Metallic Foams, Bratislava, 1–4 Sept 2009.
15. MARSAVINA L., KOVACIK J., LINUL E., *Experimental validation of micromechanical models for brittle aluminium alloy foam*, Theoretical and Applied Fracture Mechanics, **83**, pp. 11–18, 2016.
16. GIBSON L.J., ASHBY M.F., *Cellular solids*. *Structure and properties*, Second edition, The Press Syndicate of the University of Cambridge, 1997.
17. LI Q.M., MAGKIRIADIS I., HARRIGAN J.J., *Compressisive Strain at the Onset of Densification of Cellular Solids*, J. of Cellular Plastics, **42**, pp. 371–392, 2006.
18. ONCK P.R., *Application of a continuum constitutive model to metallic foam DEN-specimens in compression*, Int. J. of Mech. Sci., **43**, pp. 2947–2959, 2001.
19. KOVACIK J., MARSAVINA L., ADAMCIKOVA A., SIMANCIK F. et al., *Uniaxial compression tests of metallic foams: A Recipe*, Key Engineering Materials, **601**, pp. 237–241, 2014.
20. KOVÁCIK J., JERZ J., MINÁRIKOVÁ N., MARSAVINA L., LINUL E., *Scaling of compression strength in disordered solids: metallic foams*, Fracture and Structural Integrity, **36**, pp. 55–62, 2016.
21. PERONI M., PERONI L., AVALLE M., *The mechanical behaviour of aluminium foam structures in different loading conditions*, Int. J. of Impact Eng., **35**, pp. 644–658, 2008.
22. IRAUSQUÍN I., PÉREZ-CASTELLANOS J.L., MIRANDA V., *Evaluation of the effect of the strain rate on the compressive response of a closed-cell aluminium foam using the split Hopkinson pressure bar test*, Mat. Design, **47**, pp. 698–705, 2013.
23. SIMANČÍK F., KOVÁČIK J., SEDLIAKOVÁ N., *Deformation and Fracture Mechanism of Aluminium Foams*, Word Congress, Porous Materials (PM World Congress), October 1998, Granada, Spain, p. 245.
24. ALY M.S., *Behavior of closed cell aluminium foams upon compressive testing at elevated temperatures: Experimental results*, Materials Letters, **61**, pp. 3138–3141, 2007.
25. LINUL E., MARŞAVINA L., VOICONI T., SADOWSKI T., *Study of factors influencing the mechanical properties of polyurethane foams under dynamic compression*, Journal of Physics: Conference Series, **451**, pp. 1–6, 2013.
26. LINUL E., SERBAN D.A., VOICONI T., MARSAVINA L., SADOWSKI T., *Energy-absorption and efficiency diagrams of rigid PUR foams*, Key Engineering Materials, **601**, pp. 246–249, 2014.

Received April 12, 2016